Proceedings of the 28th IEEE
EMBS Annual International Conference
New York City, USA, Aug 30-Sept 3, 2006

Observing Frequency Content Time Evolution of Independent Hippocampal Signals

Jarno M. A. Tanskanen, *Member, IEEE*, Jarno E. Mikkonen, Jari A. K. Hyttinen, *Member, IEEE*, and Markku Penttonen

Abstract— **In this paper, we propose a method for observing frequency contents of independent hippocampal signals in time. The method is based on calculating independent component analysis (ICA) on electrophysiological multielectrode field potential measurements (MFPMs) in a running window. We have previously proposed a method for observing independently operating neural populations, i.e., functional populations (FUPOs) from MFPMs and outlined the concept, which is elaborated upon and extended in this paper, in order to facilitate analysis of functioning of the target brain area. In this paper, the proposed method is demonstrated with an example with three concurrent hippocampal measurements from an anesthetized rat brain. The proposed method can be applied in analysis of any recordings of neural networks in which contributions from a number of neural populations (NPs) are simultaneously recorded via a number of measurement points (MPs), as well in vivo as in vitro.**

I. Introduction

In this paper, we address the question of observing time evolution of the frequency contents of independent signals in hippocampus via ICA [1,2,3,4] of extracellular MFPMs. The independent signals are associated with FUPOs, which are defined as sets of neurons working in unison. Field potential (FP) measurements do not explicitly reveal single NP activity, but rather carry information on a mixture of the field potentials (FPs) from several NPs. We have previously proposed using ICA to decompose MFPMs into individual FUPOs, and a method to associate the FUPOs with their anatomical origins [5]. In the same paper, we proposed a method for observing time evolution of frequency contents of FUPOs calculated from MFPM signal pairs. In this paper, we extend the method to allow for more detailed assessment of time evolution of brain wave frequencies in several FUPOs.

The principle behind the ability to associate ICs (FUPOs) with their relative anatomical locations is to calculate ICA on several different subsets of simultaneous measurements, yielding several sets of ICs. The ICs are interpreted as FUPOs, and their spatial locations are deduced by analyzing correlations of ICs from different ICAs. To interpret the ICs correctly, they must be carefully related to the neuroanatomy. Thereafter, the FUPOs can be analyzed using any appropriate methods, e.g., time–frequency and wavelet analyses [6], and current source density analyses [7]. Any brain structure, from which MFPMs can be obtained, can be subjected to ICA FUPO analysis.

In brain research, ICA has previously been applied in a multitude of cases, including electroencephalography (EEG) [8], and EEG and magnetoencephalography (MEG) [9], and EEG, MEG, and magnetic resonance imaging analyses [10]. More closely related to our work, ICA has been used, for example, in epileptiform discharge detection from EEG [11], spike train analysis of population interactions [12], and in individual neuron action potential detection [13], but to the best of our knowledge, ICA has not been previously applied in direct analysis of MFPMs prior to [5]. We assume, that there exist a number of FUPOs, giving rise to independent measurable FUPO FPs. Extracellular MFPMs are made amongst these FUPOs, as illustrated in Fig. 1. Each MFPM MP, i.e., measurement channel, in Fig. 1A, records a different sum of the FUPO FPs. The different realization possibilities of FUPO MFPMs are illustrated in Fig. 1B through 1E.

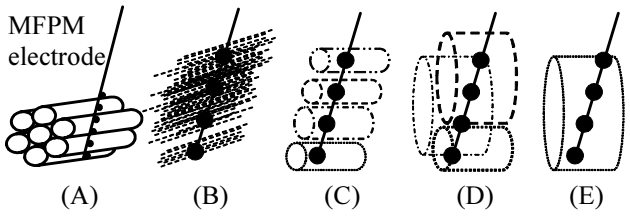

Fig. 1. (A) Illustration of an MFPM in the vicinity of FUPOs. The realization possibilities are: (B) a large number of small populations (dashed lines) in the vicinity of the MPs, (C) one population per MP, (D) each MP records contributions from one or a few FUPOs, (E) there exists one single FUPO, or any combination of (B) through (E). Dots on the MFPM shaft represent MPs, and spatial extents of measurable FUPO FPs are illustrated as cylinders.

The work of J. M. A. Tanskanen was funded by funded by Academy of Finland grant number 206996.

J. M. A. Tanskanen (phone: +358 50 387 1347; fax: +358 3 3116 4013; e-mail: tanskanen@ieee.org) and J. A. K. Hyttinen (e-mail: jari.hyttinen@tut.fi) are with Ragnar Granit Institute, Tampere University of Technology, P.O. Box 692, FI-33101 Tampere, Finland.

J. E. Mikkonen is with Department of Biological and Environmental Science and Nanoscience Center, University of Jyväskylä, P.O. Box 35, University of Jyväskylä, FI-40014 Jyväskylä, Finland (e-mail: jem@cc.jyu.fi).

M. Penttonen is with Cognitive Neurobiology Laboratory, A. I. Virtanen Institute for Molecular Sciences, University of Kuopio, P.O. Box 1627, FI-70211 Kuopio, Finland (e-mail: markku.penttonen@uku.fi).

A. Basics of ICA

In this section, basic concepts of ICA are outlined. The presentation is based on [2,3,14]. The strength of ICA lies in its ability to extract I ICs $\mathbf{x}_i$, $i = 1, 2, \ldots, I$, from J measured signals $\mathbf{y}_j$, $j = 1, 2, \ldots, J$, $I \le J$. A measured signal is assumed to be a linear combination of the ICs, $\mathbf{y}_j = a_{1,j}\mathbf{x}_1 + \ldots + a_{I,j}\mathbf{x}_I$, $j = 1, 2, \ldots, J$, where $a_{i,j}$ are coefficients of the linear combinations. Here, the measured signal $\mathbf{y}_j$ is a row vector of N voltage samples taken via one channel of several simultaneously recorded MFPM channels. In matrix form $\mathbf{Y} = \mathbf{AX}$, where measurement vectors are the rows of $\mathbf{Y}$, $\mathbf{X}$ consists of ICs in rows, and $\mathbf{A}$ is a I-by-J mixing matrix with elements $a_{i,j}$, $i = 1, 2, .., I$, $j = 1, 2, .., J$. The task of ICA is now to estimate $\mathbf{A}$, given $\mathbf{Y}$, so that the rows of $\mathbf{X}$ are independent. In order to find J ICs, at least J simultaneously recorded channels must be available. Here, $I = J = 2, 3$. Thus, ICA requires that each MFPM channel records a *linear* combination of the FUPO FPs, which may be taken sufficiently valid in order to perform the analysis. Assumptions of ICA include that 1) the components are independent, and 2) the ICs have non-Gaussian distributions. The first assumption is the essence of ICA. ICs are the maximally non-Gaussian components, and with Gaussian components, ICA is impossible. The ambiguities of ICA are that 1) energies of the found ICs cannot be determined, and 2) order of ICs is undetermined. In the sequel, ICA calculation using, e.g., two signals $\mathbf{y}_n$ and $\mathbf{y}_m$ is denoted by ICA($\mathbf{y}_n$,$\mathbf{y}_m$), and the subscript of $\mathbf{y}$ denotes the number of the MP as indicated in Fig. 2.

Here, we use a fast iterative algorithm, FastICA [3,14], available for MATLAB (MathWorks Inc., Natick, MA, USA) from the FastICA WWW site [15]. Advantages of FastICA include fast convergence, no need to set a step size parameter, tuning with respect to data by selecting a non–linearity present for the calculations [14], and one by one (as in projection pursuit) or in parallel estimation of the ICs. For most of our signals FastICA converged in a few tens of iterations, but we also encountered MFPMs for there was no converge. In such cases, turning on stabilization or using a different non–linearity in FastICA, or changing the number, length, or sampling rate of the input signals, or reducing noise, may result in convergence.

II. Multielectrode FP Measurements

Measurements presented in this paper were originally made for epilepsy research to be published elsewhere. The measurement setup is illustrated in Fig. 2. The methods used in the experiments were approved by the Provincial Government of Eastern Finland (approval number 99–61). The measurements presented in this paper are from one randomly selected rat out of a batch of 25 anaesthetized Kuopio Wistar rats. In a stereotactic instrument, a 16–channel silicon probe (courtesy of University of Michigan Center for Neural Communication Technology) with 100 μm MP separation was inserted via a drilled bone window. Recordings were made via 14 channels along the hippocampal subfields to monitor principal cell layers of dentate gyrus (DG) and Cornu Ammonis layer 1 (CA1), as well as CA1 Schaffer collaterals (Sch). Measurements via Channels 6, 8, and 15, were selected for demonstrating the proposed analysis, as they best exhibited the known characteristics of the above target cell layers. Positioning of the ME was observed from polarity of the FPs, firing patterns and population spike shapes [16], and their latencies. Two stainless steel watch screws screwed to bone above the cerebellum served as indifferent and ground electrodes. The MFPM signals were 500–fold amplified, high–pass filtered at 0.1 Hz, low–pass filtered at 5 kHz, digitized to 16–bits at 12.5 kHz sampling rate, and stored to a personal computer (PC).

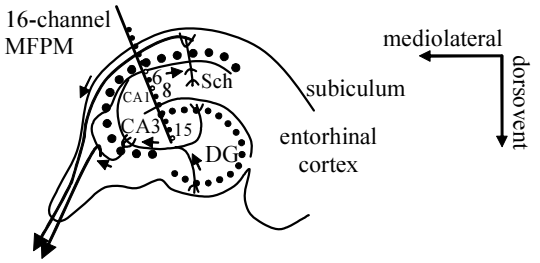

Fig. 2. Schematic illustration of the rat hippocampus –3.6 mm posterior to bregma, including an illustration of the recording electrode. Open circles on the electrode shaft illustrate the channels used in ICA, with Channel 6 (signal $\mathbf{y}_6$) in Cornu Ammonis layer 1 (CA1) pyramidal cell layer, Channel 8 (signal $\mathbf{y}_8$) amongst Schaffer collaterals (Sch), and Channel 15 (signal $\mathbf{y}_{15}$) in dentate gyrus (DG). Lines within the hippocampus illustrate fascicle, and dots the cellular layers. Cornu Ammonis layer 3 (CA3) location is also indicated.

In a PC, the sampling rate was lowered to 1562.5 Hz, and the signals were band limited within 0 Hz to 200 Hz in three steps: the signals were decimated by two, lowpass filtered using an FIR filter of length 40 (designed using window method with Hamming window to yield stopband attenuation of at least 50 dB and cutoff frequency of 200 Hz), and decimated by four. The employed decimation functions also included appropriate lowpass filters. The lowpass filtering was performed both forward and backward to preserve signal phase. Limiting the frequency band of interest below 200 Hz allows us to concentrate on FPs, and to exclude action potentials.

III. Analysis Methods

In this Section, the analysis methods are given. For frequency analysis, power spectral densities (PSDs) were calculated using the Welsh's method [17], with zero padding [18] to achieve sufficient reverberation peak frequency determination. It is to be noted that in simulations the Welch method produced untrue sidebands, and thus values less than 5 % of the maximum PSD were set to zero in all the PSD figures in this paper.

A. Deduction of FUPOs

The method to associate ICs with their anatomical FUPOs is thoroughly described in [5]. The method is based on calculating ICA on all subsets of the measurements, finding similar ICs from different ICA calculations, e.g using a clustering method or by pair wise correlations of the ICs, and thereafter deducing origins of the ICs with respect to the measured signals. The method is illustrated in Fig. 3, in which all the ICs from the ICA calculations on all the subsets of three concurrent measurements are shown. The ICs are grouped according to maximum pair wise correlation coefficients seen in Table 1. The grouping process is stopped when every IC has been assigned to a group. From the grouping results, it can be deduced that Group 1 type ICs represent the global FUPO, Group 2 ICs co-occur with $\mathbf{y}_8$ and thus represent the Sch FUPO, and finally, Group 3 ICs occur when both $\mathbf{y}_6$ and $\mathbf{y}_{15}$ are present and thus represent the CA1/DG FUPO. It may be noted that the ninth largest correlation would have associated IC_{22} with IC_{32}, with the correlation coefficient of 0.69, indicating that IC_{32} also resembles Group 3 ICs. It is to be noted that such an analysis with only a few signals may not always yield unique conclusions, and more measurements may have to be included in the analysis. The above FUPO results, and visual inspection of Group 1 and 3 ICs, suggest that there probably exists more FUPOs than observable using only three ICA input signals. Thus, to asses the true number of FUPOs and to deduce their anatomical locations, ICA might be attempted with a larger number concurrent measurements.

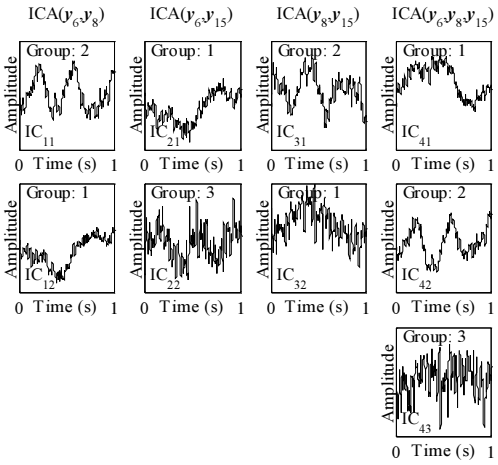

Fig. 3. ICAs of two to three MFPM signals. ICs from different ICAs are shown in columns and are individually labeled. Also shown are the grouping results deduced from the data seen in Table 1.

TABLE 1.
IC PAIRS, THEIR CORRELATION COEFFICIENTS (CC) AND THE IC GROUP NUMBERS ASSIGNED BY OBSERVING THE BEST CORRELATED IC PAIRS.

IC pair	CC	Group	IC Pair	CC	Group
IC_{12}, IC_{21}	0.98	1	IC_{12}, IC_{41}	0.89	1
IC_{31}, IC_{42}	0.94	2	IC_{22}, IC_{43}	0.84	3
IC_{21}, IC_{41}	0.91	1	IC_{11}, IC_{31}	0.83	2
IC_{11}, IC_{42}	0.89	2	IC_{32}, IC_{41}	0.71	3

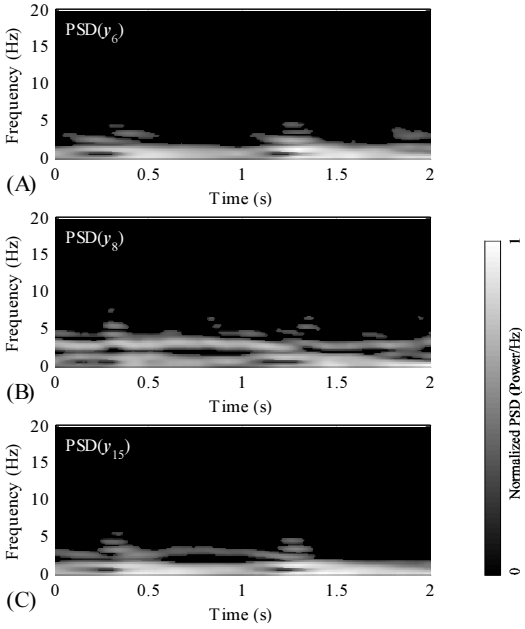

Fig. 4. PSD time series of the three original MFPMs (c.f. Fig. 2), as stated in the subfigures.

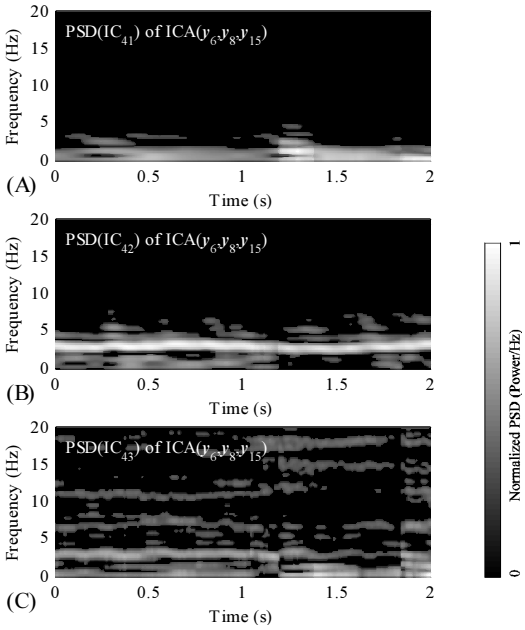

Fig. 5. PSDs three IC time series as stated in the subfigures. Note: IC_{41}, IC_{42}, and IC_{43} seen in Fig. 3, are the first ones in the IC time series used in generating the PSD time series seen in this figure, i.e., PSDs of IC_{41}, IC_{42}, and IC_{43} in Fig. 3 are seen in A, B, and C, respectively, at time 0.

B. Observing Time Evolution of Frequency Contents of the FUPOs

Observing FUPO frequency content time evolution involves the following steps:

1. Calculating ICA in a running window to produce a time series of sets of ICs.
2. Associating corresponding subsequent ICs with each other.
3. Finding the corresponding signs of the associated corresponding subsequent ICs.

4. Scaling the corresponding subsequent ICs.
5. Calculating PSDs of the ICs.
6. Plotting the PSD time series so that FUPO frequency contents are observed as functions of time.
7. Performing the reasoning described in Section IIIA in order to associate the PSD time series with the anatomical FUPOs.

In order to aid the subsequent ICA calculations to converge to similar solutions, which is necessary in order to be able to associate subsequent corresponding ICs in step 2 with each other, mixing matrix from the previous ICA calculation is to be used as an initial guess in the subsequent ICA calculation, and the ICA calculation window is to be moved in sufficiently small steps, preferably one sample at a time. Also, the window length and sampling frequency have a great effect on the success of ICA calculations, and generally have to be set by trial and error while observing the running window ICA calculations.

IV. Results

In Fig. 4, the PSD time series of three MFPM signals are shown for a two second period, and the PSD time series of the ICs from the ICA calculation using the same signals are shown in Fig. 5. When observing the PSDs of the ICs, it is to be remembered that the IC energies are indeterminate, i.e., the relative strengths of the different components cannot be assessed from Fig. 5.

Comparing the PSD time series of the original measurements in Fig. 4 with the PSD time series of the ICs in Fig. 5, it can be clearly seen that while all the original measurements exhibit somewhat similar behavior, the frequency contents of the ICs are strikingly dissimilar. This demonstrates the ability of ICA to find also the minor ICs even when buried under signals originating from stronger sources, thus possibly revealing otherwise hidden aspects of the functioning of the brain region under investigation, and the independent tasks of the associated anatomical FUPOs.

Drawing from the anatomical FUPO analysis performed in Section IIIA, it can be concluded that the slow frequency activity seen in Fig. 5A represents the global FUPO. Thereafter, theta activity seen in Fig 5B represents Sch FUPO, and finally, the high frequency activity seen in Fig. 5C can be associated with the CA1/DG FUPO.

When interpreting the results, it is to be noted that 1) while the energies of the ICs are undetermined, contributions of the ICs to the measurements can nevertheless be assessed by examining the corresponding elements of the mixing matrix **A**, and 2) thus determined minor ICs may display otherwise hard to observe information, but are also indistinguishable from colored noise.

V. Conclusion

In this paper, we have described and demonstrated a method for observing time evolution of frequency contents of independent functional populations of hippocampal neurons. The proposed method provides means for analyzing functioning of neural networks, and may be applied in various multielectrode measurement setups. The basic requirement for applying ICA is that a number of simultaneously measured signals carry linear combinations of the original source signals, i.e., FUPO FPs. This is generally well satisfied by most MFPM measurements, at least if the distance between MPs is sufficiently small. The proposed method was demonstrated by ICA of MFPMs from the rat hippocampus, and the frequency content evolution of CA1, Sch, and DG FUPOs were deduced for a continuous two second period.

References

[1] A. Hyvärinen, "Survey on independent component analysis," *Neural Computing Surveys*, vol. 2, pp. 94–128, 1999. Available: http://www.cis.hut.fi/aapo/papers/NCS99web/.

[2] A. Hyvärinen and E. Oja, "Independent component analysis: algorithms and applications," *Neural Networks*, vol. 13, pp. 411–430, June 2000.

[3] A. Hyvärinen, J. Karhunen, and E. Oja, *Independent Component Analysis*. New York, NY, USA: John Wiley & Sons, 2001.

[4] J. V. Stone, "Independent component analysis: an introduction," *Trends in Cognitive Sciences*, vol. 6, pp. 59–64, Feb. 2002.

[5] J. M. A. Tanskanen, J. E. Mikkonen, and M. Penttonen, "Independent component analysis of neural populations from multielectrode field potential measurements," *J. Neuroscience Methods*, vol. 145 pp. 213–232, June 2005. Available: http://dx.doi.org/10.1016/j.jneumeth.2005.01.004.

[6] A. Metin, Ed., *Time Frequency and Wavelets in Biomedical Signal Processing*. New York, NY, USA: IEEE Press, 1997.

[7] J. A. Freeman and C. Nicholson, "Experimental optimization of current source–density technique for anuran cerebellum," *J. Neurophysiology*, vol. 38, pp. 369–382, Mar. 1975.

[8] L. Zhukov, D. Weinstein, and C. Johnson, "Independent component analysis for EEG source localization," *IEEE Eng. Med. Biol.*, pp. 87–96, May/June 2000.

[9] R. Vigário, J. Särelä, V. Jousmäki, M. Hämäläinen, and E. Oja, "Independent component approach to the analysis of EEG and MEG recordings," *IEEE Trans. Biomed. Eng.*, vol. 47, pp. 589–593, May 2000.

[10] T.-P. Jung, S. Makeig, M. J. McKeown, A. J. Bell, T.-W. Lee, and T. J. Sejnowski, "Imaging brain dynamics using independent component analysis," *Proc. IEEE*, vol. 89, pp. 1107–1122, July 2001.

[11] K. Kobayashi, C. J. James, T. Nakahori, T. Akiyama, and J. Gotman, "Isolation of epileptiform discharges from unaveraged EEG by independent component analysis," *Clinical Neurophysiology*, vol. 110, pp. 1755–1763, Oct. 1999.

[12] M. Laubach, M. Shuler, and M. A. L. Nicolelis, "Indenpendent component analysis for quantifying neuronal ensemble interactions," *J. Neuroscience Methods*, vol. 94, pp. 141–154, Dec. 1999.

[13] G. D. Brown, S. Yamada, and T. J. Sejnowski, "Independent component analysis at the neural cocktail party," *Trends in Neurosciences*, vol. 24, pp. 54–63, Jan. 2001.

[14] A. Hyvärinen, "Fast and robust fixed–point algorithms for independent component analysis," *IEEE Trans. Neural Networks*, vol. 10, pp. 626–634, May 1999.

[15] FastICA Package for Matlab. Helsinki University of Technology: Espoo, Finland, 2005. [Online]. Available: http://www.cis.hut.fi/projects/ica/fastica/.

[16] H. Markram, J. Lübke, M. Frotscher, and B. Sakmann, "Regulation of synaptic efficacy by coincidence of postsynaptic APs and EPSPs," *Science*, vol. 275, pp. 213–215, Jan. 1997.

[17] M. H. Hayes, *Statistical Digital Signal Processing and Modeling*. New York, NY, USA: John Wiley & Sons, 1996.

[18] L. B. Jackson, *Digital Filters and Signal Processing with MATLAB Exercises*. Boston, USA: Kluwer Academic Publishers, 1996.